

# $T$ -violation in flavour oscillations as a test for relativity principles at a neutrino factory

C. N. Leung\* and Yvonne Y. Y. Wong†

*Department of Physics and Astronomy, University of Delaware, Newark, Delaware 19716*

We study the effects of violation of the equivalence principle (VEP) or violation of Lorentz invariance (LIV) in the neutrino sector on the asymmetry between  $T$ -conjugate oscillation probabilities,  $\Delta P_T \equiv P(\nu_\alpha \rightarrow \nu_\beta) - P(\nu_\beta \rightarrow \nu_\alpha)$ , in a three-flavour framework. We find that additional mixing due to these mechanisms, while obeying all present bounds, can lead to an observable enhancement, suppression, and/or sign change in  $\Delta P_T$  for the preferred energies and baselines of a neutrino factory. The measurement of this asymmetry can be used to establish a new upper limit of order  $10^{-26}$  on VEP or LIV in the  $(\nu_e, \nu_\mu)$  and  $(\nu_e, \nu_\tau)$  sectors.

## I. REVIEW AND MOTIVATIONS

The phenomenon of neutrino flavour oscillations follows from the mixing of nondegenerate neutrino states. In the “standard” scenario, a flavour neutrino is a linear combination of neutrino mass eigenstates and the degeneracy is broken by means of small neutrino masses. Alternative mechanisms that do not require neutrino masses (or more precisely, nondegenerate neutrino masses) abound. One possibility is through a violation of the equivalence principle (VEP) in the neutrino sector [1, 2]. Here, a flavour neutrino is a mixture of neutrino gravitational eigenstates and flavour-dependent neutrino-gravity couplings serve to lift the degeneracy.

An essential phenomenological difference between the standard and the VEP mechanisms is the manner in which the oscillation probability  $P(\nu_\alpha \rightarrow \nu_\beta)$  depends on the neutrino energy  $E$ . In the two-flavour case, a formal transformation from the former to the latter scenario is readily accomplished by replacing in  $P(\nu_\alpha \rightarrow \nu_\beta)$ :

$$\frac{\delta m^2}{2E} \rightarrow 2E|\phi|\delta\gamma, \quad (1)$$

where  $\delta m^2 \equiv m_2^2 - m_1^2$  is the neutrino squared mass difference,  $\delta\gamma \equiv \gamma_2 - \gamma_1$  the difference in the neutrino-gravity couplings, and  $\phi$  the Newtonian gravitational potential. Note that a violation of Lorentz invariance (LIV), where the breaking of the neutrino degeneracy is assumed by dissimilar neutrino asymptotic speeds  $v_i$  [3], may also contribute to the oscillation phenomenon with the same energy dependence as in the VEP case, save for a minor notational change:  $|\phi|\delta\gamma \rightarrow \delta v/2$ , where  $\delta v \equiv v_2 - v_1$  [4]. Henceforth, we shall use only the VEP convention.

To date, the most comprehensive set of bounds on the VEP parameter  $|\phi|\delta\gamma$  comes from the CCFR experiment [5]:  $|\phi|\delta\gamma \lesssim 10^{-22}$  for all three oscillation channels in the two-flavour limit [6]. These extremely severe constraints have since excluded VEP-LIV as an explanation

to the LSND  $\bar{\nu}_\mu \rightarrow \bar{\nu}_e$  transition puzzle [7] which requires  $|\phi|\delta\gamma \gtrsim 5 \times 10^{-18}$  [8], as well as Mikheyev-Smirnov-Wolfenstein (MSW) type solutions (with  $|\phi|\delta\gamma \gtrsim 10^{-21}$  [8, 9, 10]) to the solar neutrino problem (see later).

In the case of atmospheric  $\nu_\mu$  and  $\bar{\nu}_\mu$  disappearance, the totality of the Super-Kamiokande atmospheric neutrino data [11] strongly favours an energy dependence of  $1/E^n$ , where  $n > 0$ , in the oscillation frequency [6, 12, 13]. No acceptable VEP-LIV solution exists for the complete set of contained, partially contained, and upward going muon events. In an interesting analysis, the authors of Ref. [12] considered VEP-LIV as a sub-leading effect to standard mass-induced oscillations within a two-flavour  $\nu_\mu \leftrightarrow \nu_\tau$  framework, and derived the upper limit  $|\phi|\delta\gamma \lesssim 3 \times 10^{-24}$  at 90 % C.L. for unconstrained VEP mixing in the  $(\nu_\mu, \nu_\tau)$  sector. For maximal VEP mixing, the bound on  $|\phi|\delta\gamma$  can be as stringent as  $\sim 10^{-26}$ .

On the other hand, it has been demonstrated in a number of recent works [14, 15, 16] that vacuum oscillations induced by a “just-so” VEP with  $|\phi|\delta\gamma \sim 10^{-24}$  and  $\sin^2 2\theta \simeq 1$  can still provide a good description of the solar neutrino data [17, 18, 19, 20, 21, 22, 23]. The analyses of Ref. [15] put the solution’s goodness of fit at 60% C.L., a figure that is comparable even to the confidence level of 75 % for the standard large mixing angle (LMA) solution. However, the LMA oscillation parameters have now been confirmed by the terrestrial experiment KamLAND, through the observation of reactor  $\bar{\nu}_e$  disappearance over a typical baseline of 180 km [24]. While these new results do not exclude VEP at the aforementioned scale, a pure VEP-LIV solution to the solar  $\nu_e$  deficit is no longer justified.

It is clear from the above discussion that neutrino oscillations provide very stringent tests for the principle of equivalence and Lorentz invariance. We examine in the present work the possibility of further constraining VEP-LIV in the neutrino sector with future experiments. Currently operating long baseline terrestrial experiments (e.g., K2K), those under construction (e.g., MINOS), and prospective neutrino factories [25] will provide for us a means to obtain more precise information on the neutrino mixing properties, as well as an opportunity to establish  $CP$ - or  $T$ -violation in the lepton sector. In particular, the capacity of a neutrino factory to produce *both* elec-

\*Electronic address: leung@physics.udel.edu

†Electronic address: ywong@physics.udel.edu

tron and muon neutrino and antineutrino beams in high intensities means that it is in principle possible to directly compare the  $T$ -conjugate oscillation probabilities  $P(\nu_\mu \rightarrow \nu_e)$  and  $P(\nu_e \rightarrow \nu_\mu)$  [26]. Despite the associated experimental challenges, this is theoretically the cleanest way to resolving any  $CP$ - or  $T$ -violating phases in the neutrino mixing matrix: a nonzero measurement of  $\Delta P_T \equiv P(\nu_\alpha \rightarrow \nu_\beta) - P(\nu_\beta \rightarrow \nu_\alpha)$  necessarily implies the existence of such a phase, in contrast with the  $CP$ -asymmetry  $\Delta P_{CP} \equiv P(\nu_\alpha \rightarrow \nu_\beta) - P(\bar{\nu}_\alpha \rightarrow \bar{\nu}_\beta)$  which inevitably contains additional contribution from terrestrial matter effects.<sup>1</sup> Finally, a neutrino factory is ideal for this study since it involves high energy neutrinos travelling a very long distance, which tends to enhance the VEP-LIV effects [29].

Assuming three neutrino flavours and that standard oscillations account for both the atmospheric neutrino anomaly and solar neutrino deficit, we consider VEP-LIV as a sub-leading mechanism (while respecting all present bounds), and examine its consequence on the  $T$ -asymmetry  $\Delta P_T$  for the design parameters of a neutrino factory. We find that although the presently allowed  $|\phi|\delta\gamma$ 's are far too weak to produce any effect on the actual oscillation probabilities beyond the few percent level, the  $T$ -asymmetry can be significantly enhanced, suppressed, or flip sign, depending on the VEP-LIV breaking scale as well as the energy of the neutrinos.

We shall begin by introducing the parameters relevant for the present phenomenological study

## II. DEFINITIONS OF PHENOMENOLOGICAL PARAMETERS

Consider the evolution of a three-flavour system in a medium,

$$i \frac{d}{dt} \nu = \tilde{H} \nu, \quad (2)$$

where  $\nu = (\nu_e, \nu_\mu, \nu_\tau)^T$ . Suppose that, in addition to the usual mass-mixing and matter potential terms,  $U_M M U_M^\dagger$  and  $V$ , the total Hamiltonian  $\tilde{H}$  governing this evolution contains also a third term  $U_G G U_G^\dagger$  arising from a violation of the equivalence principle (VEP):

$$\tilde{H} = \frac{1}{2E} U_M M U_M^\dagger + 2E U_G G U_G^\dagger + V, \quad (3)$$

where

$$\begin{aligned} M &= \text{Diag}(m_1^2, m_2^2, m_3^2), \\ G &= |\phi| \times \text{Diag}(\gamma_1, \gamma_2, \gamma_3), \\ V &= \sqrt{2} G_F N_e \times \text{Diag}(1, 0, 0). \end{aligned} \quad (4)$$

Here,  $m_{1,2,3}^2$  are the squared masses of the neutrino mass eigenstates,  $\phi$  is the gravitational potential,  $\gamma_{1,2,3}$  are the neutrino-gravity couplings,  $E$  is the neutrino energy,  $G_F$  is the Fermi constant,  $N_e$  is the electron number density of the medium, and  $U_{M,G}$  are two independent unitary matrices relating the flavour eigenstates to, respectively, the mass and gravitational eigenstates. Note that the subscript capital  $M$  stands for ‘‘mass’’, and is not to be confused with the commonly used small  $m$  which denotes ‘‘matter’’.

A generic  $3 \times 3$  unimodular unitary matrix may be parameterised with three mixing angles and six phases:

$$U \equiv e^{i\eta} \text{Diag}(1, e^{i\alpha}, e^{i\beta}) U' \text{Diag}(1, e^{i\xi}, e^{i\chi}), \quad (5)$$

where  $\eta, \alpha, \beta, \xi,$  and  $\chi$  are five arbitrary phases, and the matrix  $U'$  contains the three mixing angles and the sixth phase, i.e., the  $CP$ - or  $T$ -violating phase, such as the familiar CKM matrix.<sup>2</sup> The phase  $\eta$  is an unobservable overall phase.  $\xi$  and  $\chi$  may correspond to physical Majorana phases (if neutrinos are Majorana particles), or to unphysical phases (if neutrinos are Dirac particles), neither of which contribute to flavour oscillations. If only the mass term is present, the remaining two phases  $\alpha$  and  $\beta$  are unphysical, and can always be absorbed into the definitions of the flavour eigenstates, e.g.,  $\nu'_\mu = e^{-i\alpha_M} \nu_\mu$ , leaving  $U'_M$  the only observable entity. Similarly, if  $U_G G U_G^\dagger$  is the unique term, only  $U'_G$  contributes to the oscillation phenomenon. In the general mass plus gravity case, however, it is not possible to completely eliminate the  $\alpha$  and  $\beta$  phases. If we choose  $U_M = U'_M$ , it follows that the total Hamiltonian  $\tilde{H}$  must take the form

$$\begin{aligned} \tilde{H} &= \frac{1}{2E} U'_M M U_M'^\dagger + 2E W U'_G G U_G'^\dagger W^\dagger + V \\ &\equiv H^M + W H^G W^\dagger + V \\ &\equiv H + W H^G W^\dagger, \end{aligned} \quad (6)$$

where  $W = \text{Diag}(1, e^{i\alpha}, e^{i\beta})$ , with  $\alpha \equiv \alpha_G - \alpha_M$  and  $\beta \equiv \beta_G - \beta_M$ , and we have defined  $H \equiv H^M + V$  as the ‘‘standard’’ mass-induced mixing plus matter potential sub-Hamiltonian for future reference. To transform from  $H^G$  to  $W H^G W^\dagger$ , one simply makes the following replacements:

$$\begin{aligned} H_{e\mu}^G &\rightarrow H_{e\mu}^G e^{i\alpha}, & H_{\mu e}^G &\rightarrow H_{\mu e}^G e^{-i\alpha}, \\ H_{e\tau}^G &\rightarrow H_{e\tau}^G e^{i\beta}, & H_{\tau e}^G &\rightarrow H_{\tau e}^G e^{-i\beta}, \\ H_{\mu\tau}^G &\rightarrow H_{\mu\tau}^G e^{i(\beta-\alpha)}, & H_{\tau\mu}^G &\rightarrow H_{\tau\mu}^G e^{i(\alpha-\beta)}. \end{aligned} \quad (7)$$

Thus the inclusion of a gravitational term in the total Hamiltonian leads to, in principle, eight, not six, extra observable parameters!

<sup>1</sup> It should be noted that  $T$ -violating effects can arise from an earth matter distribution that is not symmetric about the midpoint of the neutrino's trajectory, independently of the intrinsic  $CP$ - or  $T$ -violating phase [27]. See Ref. [28] for a recent study.

<sup>2</sup> A common practice is to express some of these extra phases in terms of  $SU(3)$  generators, utilising the diagonal Gell-Mann matrices  $\lambda_3$  and  $\lambda_8$ . We find our simple parameterisation to be more convenient for the present phenomenological study.

In the following, we shall make the simplifying assumption that the splitting between two of the three gravitational eigenstates is too small to be probed by present day experiments and experiments in the near future. This near degeneracy means that only one  $|\phi|\delta\gamma$  and two VEP mixing angles contribute to the observable part of  $H^G$ , and the  $CP$ - or  $T$ -violating phase inherent in  $U'_G$  can be absorbed into the definitions of the phases  $\alpha$  and  $\beta$ . We shall adopt the convention  $\gamma_1 \simeq \gamma_2$  and  $\delta\gamma \equiv \gamma_3 - \gamma_2$ , and parameterise the effective  $U'_G$  as

$$U'_G = \begin{pmatrix} \cos\varphi & 0 & \sin\varphi \\ -\sin\psi \sin\varphi & \cos\psi & \sin\psi \cos\varphi \\ -\cos\psi \sin\varphi & -\sin\psi & \cos\psi \cos\varphi \end{pmatrix}, \quad (8)$$

where  $\varphi$  and  $\psi$  run from  $-\pi/2$  to  $\pi/2$ . The resulting three-flavour sub-Hamiltonian  $H^G$  takes the form

$$E|\phi|\delta\gamma \begin{pmatrix} 2\sin^2\varphi & \sin\psi \sin 2\varphi & \cos\psi \sin 2\varphi \\ \sin\psi \sin 2\varphi & 2\cos^2\varphi \sin^2\psi & \cos^2\varphi \sin 2\psi \\ \cos\psi \sin 2\varphi & \cos^2\varphi \sin 2\psi & 2\cos^2\varphi \cos^2\psi \end{pmatrix}, \quad (9)$$

which reduces to a pure two-flavour description in terms of one mixing angle when either  $\varphi$  or  $\psi$  is fixed at 0,  $\pi/2$ , or  $-\pi/2$ . Specifically

$$\begin{aligned} \sin^2\psi = 1 &\Rightarrow \nu_e \leftrightarrow \nu_\mu \text{ VEP mixing,} \\ \sin^2\psi = 0 &\Rightarrow \nu_e \leftrightarrow \nu_\tau \text{ VEP mixing,} \\ \sin^2\varphi = 0 &\Rightarrow \nu_\mu \leftrightarrow \nu_\tau \text{ VEP mixing.} \end{aligned} \quad (10)$$

Observe that the sign of the parameter  $|\phi|\delta\gamma$  may be positive or negative. As we shall see, this has important consequences when considered together with  $H^M + V$ .

For the mass-mixing term  $H^M$ , we adopt the usual MNS parameterisation [30] for  $U'_M$ :

$$U'_M = \begin{pmatrix} c_1 c_3 & s_1 c_3 & s_3 e^{-i\delta} \\ -s_1 c_2 - c_1 s_2 s_3 e^{i\delta} & c_1 c_2 - s_1 s_2 s_3 e^{i\delta} & s_2 c_3 \\ s_1 s_2 - c_1 c_2 s_3 e^{i\delta} & -c_1 s_2 - s_1 c_2 s_3 e^{i\delta} & c_2 c_3 \end{pmatrix}, \quad (11)$$

where  $s_i \equiv \sin\theta_i$ ,  $c_i \equiv \cos\theta_i$ ,  $i = 1, 2, 3$ , and  $\delta$  is the  $CP$ - or  $T$ -violating phase. The solar and atmospheric oscillation parameters are identified as

$$\begin{aligned} \delta m_{\text{atm}}^2 &\equiv \delta m_{32}^2 \equiv m_3^2 - m_2^2, & \theta_{\text{atm}} &\equiv \theta_2, \\ \delta m_{\text{sun}}^2 &\equiv \delta m_{21}^2 \equiv m_2^2 - m_1^2, & \theta_{\text{sun}} &\equiv \theta_1, \end{aligned} \quad (12)$$

assuming that maximal  $\nu_\mu \leftrightarrow \nu_\tau$  oscillations with  $\delta m_{\text{atm}}^2 \simeq 3 \times 10^{-3} \text{ eV}^2$ , and the large mixing angle (LMA) solution ( $\delta m_{\text{sun}}^2 \simeq 5 \times 10^{-5} \text{ eV}^2$ ,  $\sin 2\theta_{\text{sun}} \simeq 0.8$ ) explain, respectively, the atmospheric and solar neutrino anomalies. Given these solutions, a three-flavour analysis of the CHOOZ data sees the remaining angle  $\theta_3$  constrained to  $\tan^2\theta_3 < 0.055$  at 90% C.L. [31].

### III. WHY $T$ -VIOLATION EXPERIMENTS?

Solution to the Hamiltonian (3) may be obtained by first transforming to a new basis defined as

$$\tilde{U}^\dagger \tilde{H} \tilde{U} = \text{Diag}(\tilde{\lambda}_1, \tilde{\lambda}_2, \tilde{\lambda}_3), \quad (13)$$

where  $\tilde{\lambda}_{1,2,3}$  are the eigenvalues, and the energy dependent unitary matrix  $\tilde{U}$  contains by definition one independent effective  $CP$ - or  $T$ -violating phase. Assuming constant  $N_e$  and  $\phi$ , the asymmetry between the  $T$ -conjugate oscillation probabilities  $\tilde{P}(\nu_\alpha \rightarrow \nu_\beta)$  and  $\tilde{P}(\nu_\beta \rightarrow \nu_\alpha)$  is given by

$$\begin{aligned} \Delta\tilde{P}_T &\equiv \tilde{P}(\nu_\alpha \rightarrow \nu_\beta) - \tilde{P}(\nu_\beta \rightarrow \nu_\alpha) \\ &= 16\tilde{J} \sin \frac{\tilde{\Delta}_{12}L}{2} \sin \frac{\tilde{\Delta}_{23}L}{2} \sin \frac{\tilde{\Delta}_{31}L}{2}, \end{aligned} \quad (14)$$

where  $\tilde{\Delta}_{ij} \equiv \tilde{\lambda}_i - \tilde{\lambda}_j$ , with  $i, j = 1, 2, 3$ , is the difference between the  $i$ th and the  $j$ th eigenvalues, and

$$\tilde{J} \equiv \tilde{J}_{\alpha\beta}^{ij} = \text{Im}(\tilde{U}_{\beta i} \tilde{U}_{\beta j}^* \tilde{U}_{\alpha i}^* \tilde{U}_{\alpha j}) \quad (15)$$

is the effective Jarlskog factor [32] encapsulating the said effective phase.

Explicit evaluation of the quantities  $\tilde{J}$  and  $\tilde{\Delta}_{ij}$  is a tedious, though straightforward, task. Fortunately, there exists a very useful identity which relates them to the original Hamiltonian in flavour space [33]:

$$\tilde{\Delta}_{12}\tilde{\Delta}_{23}\tilde{\Delta}_{31}\tilde{J} = \text{Im}(\tilde{H}_{e\mu}\tilde{H}_{\mu\tau}\tilde{H}_{\tau e}). \quad (16)$$

Observe that (i) the right hand side of Eq. (16) is dependent only on the off-diagonal elements of  $\tilde{H}$ , and (ii) the left hand side of Eq. (16) bears a striking resemblance to the right hand side of Eq. (14). These immediately suggest that the observable  $\Delta\tilde{P}_T$  is potentially very sensitive to the additional mixing terms arising from VEP.

We do not consider the  $CP$  asymmetry  $\Delta\tilde{P}_{CP} \equiv \tilde{P}(\nu_\alpha \rightarrow \nu_\beta) - \tilde{P}(\bar{\nu}_\alpha \rightarrow \bar{\nu}_\beta)$  in the present work. This measurable inevitably contains additional contribution from terrestrial matter effects, thus rendering its analytical description much more complicated.

## IV. ANALYSIS

We now analyse the effects of VEP on the observed  $T$ -asymmetry. Consider the ratio

$$\frac{\Delta\tilde{P}_T}{\tilde{P}_T} = \frac{\tilde{J} \sin \frac{\tilde{\Delta}_{12}L}{2} \sin \frac{\tilde{\Delta}_{23}L}{2} \sin \frac{\tilde{\Delta}_{31}L}{2}}{J \sin \frac{\Delta_{12}L}{2} \sin \frac{\Delta_{23}L}{2} \sin \frac{\Delta_{31}L}{2}}, \quad (17)$$

where the quantities with a tilde are as defined in Eqs. (14) and (15), and those without correspond to their ‘‘standard’’  $H^G = 0$  counterparts. Using the matter-invariants

$$\text{Im}(H_{e\mu}H_{\mu\tau}H_{\tau e}) = \text{Im}(H_{e\mu}^M H_{\mu\tau}^M H_{\tau e}^M), \quad (18)$$

and

$$J = \frac{1}{8E^3} \frac{\delta m_{12}^2 \delta m_{23}^2 \delta m_{31}^2}{\Delta_{12}\Delta_{23}\Delta_{31}} J^M, \quad (19)$$

where

$$J^M = s_1 c_1 s_2 c_2 s_3 c_3^2 \sin \delta \quad (20)$$

is the Jarlskog factor in vacuum, we rewrite Eq. (17) as

$$\frac{\Delta \tilde{P}_T}{\Delta P_T} = \frac{8E^3 \Delta_{12} \Delta_{23} \Delta_{31} \tilde{J}}{\delta m_{12}^2 \delta m_{23}^2 \delta m_{31}^2 J^M} \times \left( \frac{\sin \frac{\tilde{\Delta}_{12} L}{2}}{\sin \frac{\Delta_{12} L}{2}} \frac{\sin \frac{\tilde{\Delta}_{23} L}{2}}{\sin \frac{\Delta_{23} L}{2}} \frac{\sin \frac{\tilde{\Delta}_{31} L}{2}}{\sin \frac{\Delta_{31} L}{2}} \right). \quad (21)$$

Rough estimates of the differences between the eigenvalues  $\tilde{\Delta}_{ij}$ ,  $ij = 12, 23, 31$  may be extracted from the Hamiltonian (3) and Eq. (4):

$$\tilde{\Delta}_{12} \simeq \frac{m_1^2 - m_2^2}{2E} + \mathcal{O}(\sqrt{2}G_F N_e) + \mathcal{O}(2E|\phi|\delta\gamma), \quad (22)$$

$$\tilde{\Delta}_{23} \simeq \frac{m_2^2 - m_3^2}{2E} + \mathcal{O}(2E|\phi|\delta\gamma), \quad (23)$$

$$\tilde{\Delta}_{31} \simeq \frac{m_3^2 - m_1^2}{2E} - \mathcal{O}(\sqrt{2}G_F N_e) + \mathcal{O}(2E|\phi|\delta\gamma). \quad (24)$$

Their standard counterparts  $\Delta_{ij}$  are given similarly, save for the absence of the  $\mathcal{O}(2E|\phi|\delta\gamma)$  terms.

Suppose now that

$$2E|\phi|\delta\gamma \ll \frac{|\delta m_{32}^2|}{2E}, \quad (25)$$

or, equivalently,

$$|\phi|\delta\gamma \ll 2.5 \times 10^{-19} \frac{|\delta m_{32}^2|}{\text{eV}^2} \left( \frac{\text{GeV}}{E} \right)^2. \quad (26)$$

This immediately allows us to set  $\tilde{\Delta}_{23} \simeq \Delta_{23}$ , and thus

$$\sin \frac{\tilde{\Delta}_{23} L}{2} \simeq \sin \frac{\Delta_{23} L}{2}. \quad (27)$$

For  $|\delta m_{32}^2| \simeq 3 \times 10^{-3} \text{ eV}^2$ , and a neutrino factory producing a neutrino beam of average energy 13 GeV, Eq. (25) is a good approximation for  $|\phi|\delta\gamma \ll 4 \times 10^{-24}$ , a region of parameter space well below the present CCFR bounds. Further approximations are in line, depending on whether  $\tilde{\Delta}_{31}$  is *on-* or *off-resonance*.

*Off-resonance:*  $\tilde{\Delta}_{31} \neq 0$ . If there is no exact or near cancellation between  $\mathcal{O}(\sqrt{2}G_F N_e)$  and other terms in Eq. (24), the condition (25) implies also that  $\tilde{\Delta}_{31} \simeq \Delta_{31}$ , and therefore

$$\sin \frac{\tilde{\Delta}_{31} L}{2} \simeq \sin \frac{\Delta_{31} L}{2}. \quad (28)$$

Hence,

$$\frac{\Delta \tilde{P}_T}{\Delta P_T} \simeq \frac{8E^3 \Delta_{12} \tilde{\Delta}_{23} \tilde{\Delta}_{31} \tilde{J}}{\delta m_{12}^2 \delta m_{23}^2 \delta m_{31}^2 J^M} \frac{\sin \frac{\tilde{\Delta}_{12} L}{2}}{\sin \frac{\Delta_{12} L}{2}}, \quad (29)$$

and only  $\tilde{\Delta}_{12}$  is substantially affected by  $H^G$ . Equation (29) may be further simplified if the neutrino energy and the experimental baseline are such that

$$\sin \frac{\tilde{\Delta}_{12} L}{2} \simeq \frac{\tilde{\Delta}_{12} L}{2}, \quad \sin \frac{\Delta_{12} L}{2} \simeq \frac{\Delta_{12} L}{2}, \quad (30)$$

or, roughly speaking, if the experimental baseline satisfies the requirement

$$L < \frac{2}{|\tilde{\Delta}_{12}|} \simeq \frac{2}{\text{Max} \left( \frac{\delta m_{21}^2}{2E}, \sqrt{2}G_F N_e, 2E|\phi|\delta\gamma \right)}. \quad (31)$$

The outcome of this approximation is a  $T$ -asymmetry ratio that is related in a simple way to the off-diagonal elements of the original Hamiltonians in flavour space,

$$\frac{\Delta \tilde{P}_T}{\Delta P_T} \simeq \frac{8E^3 \tilde{\Delta}_{12} \tilde{\Delta}_{23} \tilde{\Delta}_{31} \tilde{J}}{\delta m_{12}^2 \delta m_{23}^2 \delta m_{31}^2 J^M} = \frac{\text{Im}(\tilde{H}_{e\mu} \tilde{H}_{\mu\tau} \tilde{H}_{\tau e})}{\text{Im}(H_{e\mu}^M H_{\mu\tau}^M H_{\tau e}^M)}, \quad (32)$$

independently of the baseline of the experiment. This is one of the main results of the present work.

*On-resonance:*  $\tilde{\Delta}_{31} \simeq 0$ . The near cancellation of  $\mathcal{O}(\sqrt{2}G_F N_e)$  with other terms in Eq. (24) and the condition (25) together imply for Eq. (22) that

$$\tilde{\Delta}_{12} \simeq \frac{m_3^2 - m_2^2}{2E} + \mathcal{O}(2E|\phi|\delta\gamma) \simeq \Delta_{12}, \quad (33)$$

and thus

$$\sin \frac{\tilde{\Delta}_{12} L}{2} \simeq \sin \frac{\Delta_{12} L}{2}. \quad (34)$$

Furthermore, if the experimental baseline and the neutrino energy satisfy the condition

$$L < \frac{2}{|\tilde{\Delta}_{31}|} \simeq \frac{2}{\text{Max} \left( \frac{|\delta m_{31}^2|}{2E} \sin 2\theta_3, 2E|\phi|\delta\gamma \right)}, \quad (35)$$

then the approximations

$$\sin \frac{\tilde{\Delta}_{31} L}{2} \simeq \frac{\tilde{\Delta}_{31} L}{2}, \quad \sin \frac{\Delta_{31} L}{2} \simeq \frac{\Delta_{31} L}{2} \quad (36)$$

are also well-founded. Substituting Eqs. (27), (34) and (36) into Eq. (17), we find that the  $T$ -asymmetry ratio in the on-resonance case is equally well described by Eq. (32), except for a different baseline requirement (35).

As it turns out, Eq. (32) is a generally valid approximation for the preferred parameters of a neutrino factory: an average neutrino energy of about 10 to 30 GeV and a baseline roughly between 3000 and 6000 km, provided that Eq. (25) holds.

It is useful to rewrite Eq. (32) as

$$\frac{\Delta \tilde{P}_T}{\Delta P_T} \equiv 1 + R, \quad (37)$$

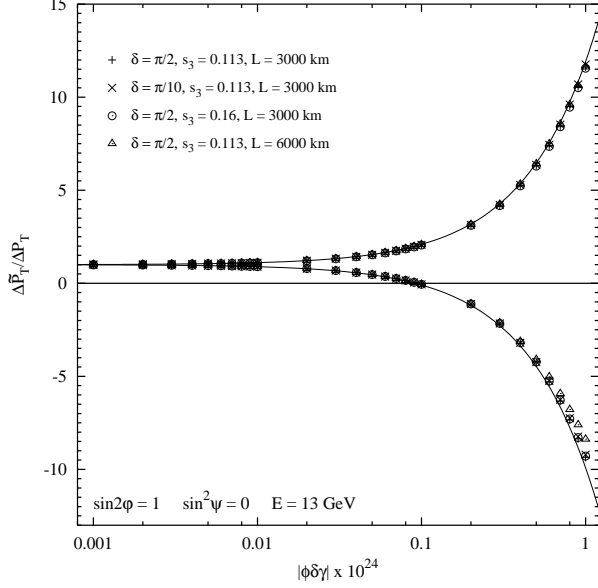


FIG. 1:  $\Delta\tilde{P}_T/\Delta P_T$  versus  $|\phi|\delta\gamma$  for  $E = 13$  GeV, maximal  $\nu_e \leftrightarrow \nu_\tau$  VEP mixing ( $\sin 2\varphi = 1$  and  $\sin^2 \psi = 0$ ), and with the relative phase  $\beta$  set to zero. The standard oscillation parameters used here are the best fit values:  $|\delta m_{32}^2| = 3 \times 10^{-3} \text{ eV}^2$ ,  $\sin 2\theta_2 = 1$ ,  $\delta m_{21}^2 = 5 \times 10^{-5} \text{ eV}^2$ , and  $\sin 2\theta_1 = 0.8$ . The four sets of points correspond to exact values of  $\Delta\tilde{P}_T/\Delta P_T$  from numerical calculations for different values of  $s_3$ ,  $\delta$ , and baselines  $L$ . The solid lines come from the approximate equation (43); the top (bottom) set is for negative (positive)  $|\phi|\delta\gamma$ 's.

with

$$R \simeq \sum_{ijk}^{\text{cyclic}} \left[ \frac{\text{Im}(H_{ij}^M H_{jk}^M H_{ki}^{G'})}{\text{Im}(H_{e\mu}^M H_{\mu\tau}^M H_{\tau e}^M)} + \frac{\text{Im}(H_{ij}^{G'} H_{jk}^{G'} H_{ki}^M)}{\text{Im}(H_{e\mu}^M H_{\mu\tau}^M H_{\tau e}^M)} \right], \quad (38)$$

where  $H_{ij}^{G'} \equiv (WH^G W^\dagger)_{ij}$ , the summation is taken over  $ijk = e\mu\tau, \mu\tau e, \tau e\mu$ , and we have used

$$\text{Im}(H_{e\mu}^{G'} H_{\mu\tau}^{G'} H_{\tau e}^{G'}) = \text{Im}(H_{e\mu}^G H_{\mu\tau}^G H_{\tau e}^G) = 0, \quad (39)$$

since two of the three gravitational eigenstates are by assumption degenerate. The five extra parameters from  $H^{G'}$  offer a plethora of possibilities. We provide here a few illustrative cases, but the list is by no means exhaustive.

### A. Pure $\nu_e \leftrightarrow \nu_\tau$ VEP mixing

The setting of  $\psi = 0$  corresponds to pure  $\nu_e \leftrightarrow \nu_\tau$  mixing in the VEP sector. In Eq. (38), the only surviving term is

$$R \simeq \frac{\text{Im}(H_{e\mu}^M H_{\mu\tau}^M H_{\tau e}^{G'})}{\text{Im}(H_{e\mu}^M H_{\mu\tau}^M H_{\tau e}^M)}. \quad (40)$$

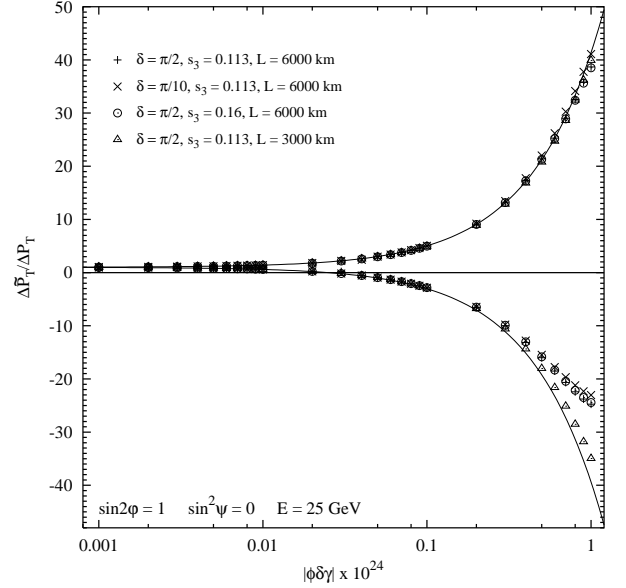


FIG. 2: Same as Fig. 1, except for  $E = 25$  GeV.

Using the parameterisation introduced in Sec. II, we obtain

$$\frac{\Delta\tilde{P}_T}{\Delta P_T} \simeq 1 + \frac{2E^2 B}{\delta m_{21}^2} |\phi|\delta\gamma \sin 2\varphi, \quad (41)$$

where

$$B \simeq \frac{s_2}{s_1 c_1} \frac{\sin(\beta - \delta)}{\sin \delta} \left( 1 + \frac{\delta m_{21}^2}{\delta m_{32}^2} \right) + \frac{c_2}{s_3} \frac{\delta m_{21}^2}{\delta m_{32}^2} \frac{\sin \beta}{\sin \delta}, \quad (42)$$

to leading order in  $(\delta m_{21}^2/\delta m_{32}^2)$  and  $s_3$ . As expected, the increment  $R$  scales with the square of the neutrino energy  $E^2$  and the VEP breaking scale  $|\phi|\delta\gamma$  which may be positive or negative. Since we have restricted  $|\phi|\delta\gamma$  to be much smaller than the atmospheric oscillation scale [Eq. (25)],  $|\phi|\delta\gamma$  interferes substantially only with the solar neutrino mass splitting  $\delta m_{21}^2$ , and hence only  $\delta m_{21}^2$  appears in the leading order term of  $R$ . Naturally, the degree of  $\nu_e \leftrightarrow \nu_\tau$  VEP mixing,  $\sin 2\varphi$ , is also a contributing factor.

The quantity  $B$  depends on the mixing angles of  $U_M$  (some of which we assume can be established from existing experimental data), as well as the intrinsic  $CP$  phase  $\delta$  and one of the relative phases  $\beta$ . In the simplest case where  $\beta = 0$ ,  $B$  becomes independent of both  $\theta_3$  and  $\delta$  such that

$$\frac{\Delta\tilde{P}_T}{\Delta P_T} \simeq 1 - \frac{4E^2}{\delta m_{21}^2} \frac{\sin \theta_2}{\sin 2\theta_1} |\phi|\delta\gamma \sin 2\varphi, \quad (43)$$

to zeroth order in  $(\delta m_{21}^2/\delta m_{32}^2)$ . Figure 1 shows the approximate equation (43) plotted as a function of  $|\phi|\delta\gamma$  with the neutrino energy fixed at 13 GeV for maximal VEP mixing,  $\sin 2\varphi = 1$ . Also displayed in juxtaposition are four sets of data points corresponding to exact

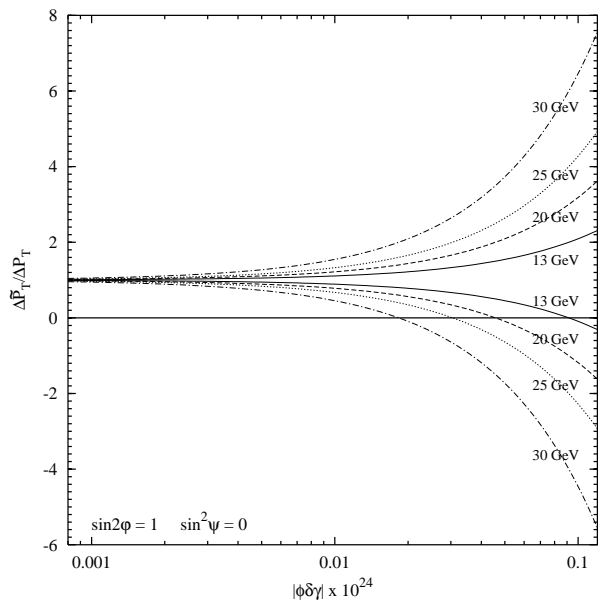


FIG. 3:  $\Delta\tilde{P}_T/\Delta P_T$  versus  $|\phi|\delta\gamma$  for different neutrino energies. Maximal  $\nu_e \leftrightarrow \nu_\tau$  VEP mixing is assumed, and  $\beta = 0$ . The top (bottom) set of curves is for negative (positive)  $|\phi|\delta\gamma$ 's. We use the best-fit standard oscillation parameters and  $s_3 = 0.113$ .

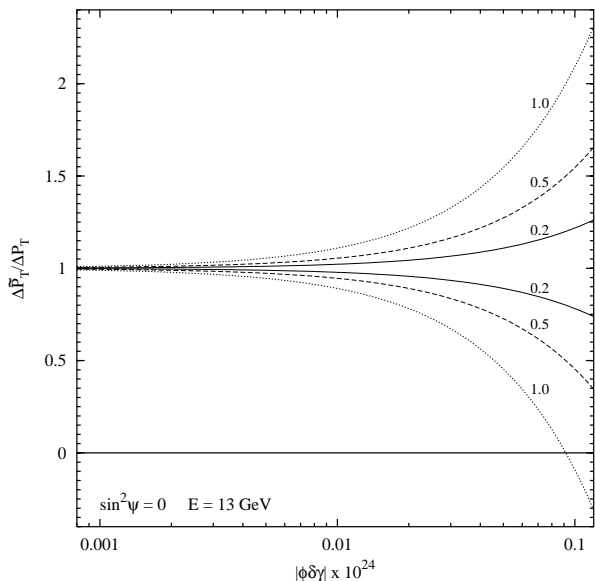


FIG. 4:  $\Delta\tilde{P}_T/\Delta P_T$  versus  $|\phi|\delta\gamma$  for different values of  $\sin 2\varphi$ , while  $\sin^2 \psi$  and  $\beta$  are set to zero, and the neutrino energy is fixed at 13 GeV. The top (bottom) set of curves is for negative (positive)  $|\phi|\delta\gamma$ 's.

values of  $\Delta\tilde{P}_T/\Delta P_T$  calculated numerically for different values of  $s_3$ ,  $\delta$ , and baselines  $L$ . Figure 2 is similar to Fig. 1, save for a different neutrino energy,  $E = 25$  GeV. Concordance between the exact and the approximate results generally obtains. Deviations from the exact results appear for the larger  $|\phi|\delta\gamma$ 's ( $\gtrsim 10^{-25}$ ) as one tunes up

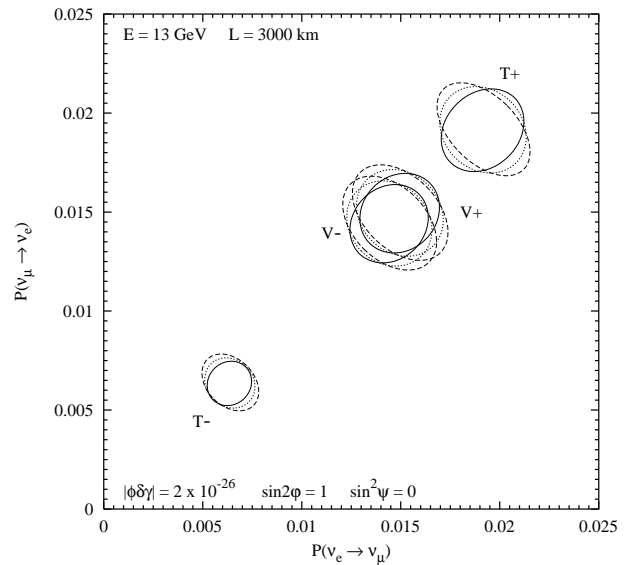


FIG. 5:  $T$ -trajectory diagram for maximal  $\nu_e \leftrightarrow \nu_\tau$  VEP mixing, with  $\beta = 0$ . The ellipses labelled  $V+$  ( $-$ ) are the trajectories in vacuum for a positive (negative)  $\delta m_{32}^2$ . Those labelled  $T+$  and  $T-$  are the corresponding trajectories in matter. Solid (dashed) lines are for a positive (negative)  $|\phi|\delta\gamma$ , while dotted lines are for the standard, no VEP case.

the neutrino energy, since satisfaction of the requirement (25) becomes increasingly poor.

Depending on the relative sign of  $|\phi|\delta\gamma$  and  $\delta m_{21}^2$ , the ratio  $\Delta\tilde{P}_T/\Delta P_T$  splits into two branches for any given set of  $E$  and  $\sin 2\varphi$ . Since the sign of  $\delta m_{21}^2$  is fixed by the solar neutrino data to be positive, the dependence is on the sign of  $|\phi|\delta\gamma$  only, as is evident in Figs. 1 and 2. The top branch, where  $|\phi|\delta\gamma < 0$ , always leads to an enhancement in the observed  $T$ -asymmetry. The bottom branch, on the other hand, shows a  $\Delta\tilde{P}_T/\Delta P_T$  that tends to zero, flips sign, and then continues to grow in magnitude as we increase  $|\phi|\delta\gamma$ .

More  $\Delta\tilde{P}_T/\Delta P_T$  versus  $|\phi|\delta\gamma$  curves are displayed in Figs. 3 and 4, for different neutrino energies and mixing parameters  $\sin 2\varphi$ . Figure 3 shows that deviations of  $\Delta\tilde{P}_T$  from  $\Delta P_T$  are more prominent for higher energy neutrinos, which is consistent with expectation. Depending on the neutrino energy, the enhancement in the magnitude of the  $T$ -asymmetry in the parameter region  $10^{-26} \lesssim |\phi|\delta\gamma \lesssim 10^{-25}$  can be anywhere from  $\sim 20\%$  to a factor of a few.

It is interesting to note that the corresponding changes in the actual oscillation probabilities are generally no more than a few percent, as illustrated, for example, by the  $T$ -trajectory diagrams in Fig. 5.<sup>3</sup> Thus, by comparing the appearance rates of two  $T$ -conjugate channels,

<sup>3</sup>  $CP$ - and  $T$ -trajectory diagrams were first introduced in Refs. [34] and [35] respectively.

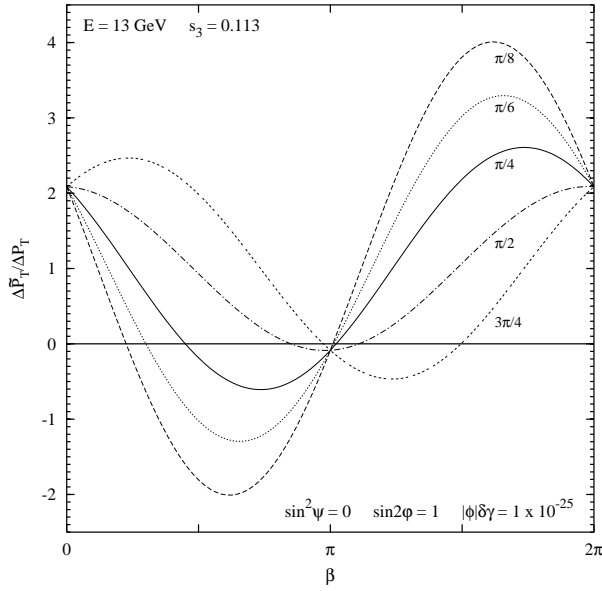


FIG. 6:  $\Delta\tilde{P}_T/\Delta P_T$  versus  $\beta$  for different values of  $\delta$  for maximal  $\nu_e \leftrightarrow \nu_\tau$  VEP mixing. The neutrino energy is fixed at 13 GeV and  $|\phi|\delta\gamma = 1 \times 10^{-25}$ .

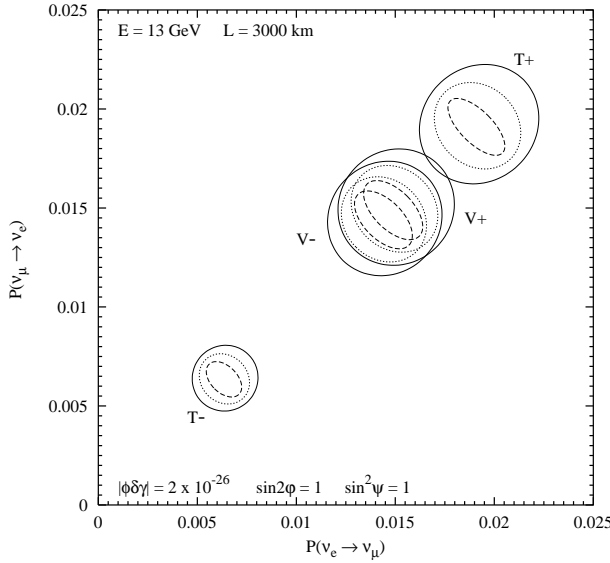


FIG. 7: Same as Fig. 5, but for maximal  $\nu_e \leftrightarrow \nu_\mu$  VEP mixing and  $\alpha = 0$ .

we will be able to probe a whole new region of VEP parameter space that is inaccessible to conventional single channel appearance or disappearance experiments run at the same energies.

Before concluding this section, let us remark on the relative phase  $\beta$ . Figure 6 shows  $\Delta\tilde{P}_T/\Delta P_T$  as a function of  $\beta$ , according to Eqs. (41) and (42), for several values of  $\delta$ 's at a fixed  $E^2|\phi|\delta\gamma \sin 2\varphi$ . The message here is clear: extra phases in the Hamiltonian do not always contribute to increasing the extent of  $T$ -violation, particularly when  $\delta$  is already close to the maximally  $T$ -violating value of

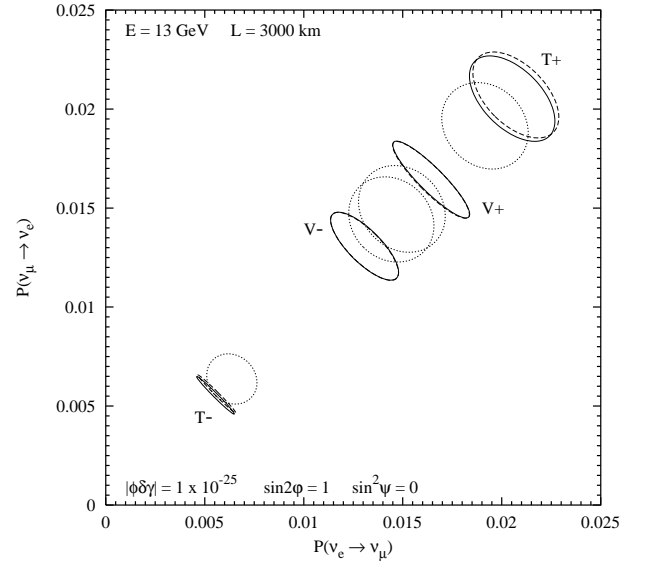


FIG. 8:  $T$ -trajectory diagram for maximal  $\nu_e \leftrightarrow \nu_\tau$  VEP mixing with  $\beta$  as the phase variable. The standard  $CP$  phase  $\delta$  is set to identically zero. The ellipses labelled  $V+$  ( $-$ ) are the trajectories in vacuum for a positive (negative)  $\delta m_{32}^2$ . Those labelled  $T+$  and  $T-$  are the corresponding trajectories in matter. Solid (dashed) lines are for a positive (negative)  $|\phi|\delta\gamma$ . For the purpose of comparison, we have also included the standard  $T$ -trajectories (as functions of  $\delta$ ). These are represented by the dotted lines.

$\pi/2$  or  $3\pi/2$ . Interference between the phases means that the final  $T$ -asymmetry may even be suppressed to zero. On the other hand, if  $|\sin \delta| \ll |\sin \beta|$ , the latter becomes the dominant phase, and the  $T$ -asymmetry generated therefrom peaks at  $\beta \simeq \pi/2, 3\pi/2$ , as is evident in Fig. 6. We will revisit this issue in a later section.

## B. Pure $\nu_e \leftrightarrow \nu_\mu$ VEP mixing

This case corresponds to setting  $\psi = \pi/2$ . The  $T$ -asymmetry ratio is given by

$$\frac{\Delta\tilde{P}_T}{\Delta P_T} \simeq 1 + \frac{2E^2 A}{\delta m_{21}^2} |\phi|\delta\gamma \sin 2\varphi, \quad (44)$$

where

$$A \simeq \frac{c_2}{s_1 c_1} \frac{\sin(\delta - \alpha)}{\sin \delta} \left( 1 + \frac{\delta m_{21}^2}{\delta m_{32}^2} \right) + \frac{s_2}{s_3} \frac{\delta m_{21}^2}{\delta m_{32}^2} \frac{\sin \alpha}{\sin \delta}, \quad (45)$$

to leading order in  $(\delta m_{21}^2/\delta m_{32}^2)$  and  $s_3$ . Comparing Eqs. (42) and (45), we see that since  $s_2 \simeq c_2 \simeq 1/\sqrt{2}$ , the effects of this VEP mixing channel on the  $T$ -asymmetry must be very similar to those from pure  $\nu_e \leftrightarrow \nu_\tau$  VEP mixing. In the case of  $\alpha = \beta = 0$ , the changes induced in  $\Delta\tilde{P}_T$  are identical for the two mixing channels upon replacing  $|\phi|\delta\gamma \rightarrow -|\phi|\delta\gamma$  in Eq. (44). The actual oscillation probabilities, however, are quite different. Compare the  $T$ -trajectories in Fig. 7 with those in Fig. 5.

### C. Pure $\nu_\mu \leftrightarrow \nu_\tau$ VEP mixing

The case of  $\nu_\mu \leftrightarrow \nu_\tau$  mixing is equivalent to setting  $\varphi = 0$ , such that

$$\frac{\Delta\tilde{P}_T}{\Delta P_T} \simeq 1 + \frac{2E^2 C}{\delta m_{21}^2} |\phi| \delta \gamma \sin 2\psi, \quad (46)$$

where

$$C \simeq -\frac{1}{s_2 c_2} \frac{\delta m_{21}^2}{\delta m_{32}^2} \frac{s_2^2 \sin(\alpha - \beta - \delta) - c_2^2 \sin(\alpha - \beta + \delta)}{\sin \delta} + \frac{s_3}{s_1 c_1} \frac{\sin(\alpha - \beta)}{\sin \delta} \quad (47)$$

is suppressed by a factor of  $(\delta m_{21}^2/\delta m_{32}^2)$  or  $s_3$ . This implies that the magnitude of the increment  $R$  is generally some  $\mathcal{O}(10^{-1}) \rightarrow \mathcal{O}(10^{-2})$  times smaller than would be observed in the case of, say, pure  $\nu_e \leftrightarrow \nu_\tau$  VEP mixing for the same  $|\phi|\delta\gamma$  and mixing parameter, and at the same energy. At  $E = 13$  GeV and  $|\phi|\delta\gamma \sim 10^{-25}$ , the change in the  $T$ -asymmetry is no more than one per cent, unless  $|\sin \delta| \ll |\sin(\alpha - \beta)|$ . Thus  $T$ -violation experiments run at energies of a few tens GeV are unable to probe VEP in the  $(\nu_\mu, \nu_\tau)$  sector to below  $\sim 10^{-24}$ , let alone supersede the  $|\phi|\delta\gamma \lesssim 10^{-26}$  bound imposed by the Super-Kamiokande atmospheric neutrino data [12].

### V. $T$ -VIOLATION WITH $\delta = 0$

An interesting consequence of a nonzero  $\alpha$  and/or  $\beta$  is that either or both of these relative phases alone can give rise to  $T$ -violation in the oscillation probabilities, in the absence of any explicit  $CP$ - or  $T$ -violating phases in the mixing matrices  $U'_M$  and  $U'_G$ . Consider for example VEP mixing only in the  $(\nu_e, \nu_\tau)$  sector, i.e.,  $\psi = 0$ . From Eqs. (41) and (42), the asymmetry  $\Delta\tilde{P}_T$  is given approximately by

$$\Delta\tilde{P}_T \simeq Q \sin \beta \times \left\{ 16 s_1 c_1 s_2 c_2 s_3 c_3^2 \left[ \frac{1}{8E^3} \frac{\delta m_{12}^2 \delta m_{23}^2 \delta m_{31}^2}{\Delta_{12} \Delta_{23} \Delta_{31}} \right] \times \sin \frac{\Delta_{12} L}{2} \sin \frac{\Delta_{23} L}{2} \sin \frac{\Delta_{31} L}{2} \right\}, \quad (48)$$

where

$$Q = \frac{2E^2 |\phi| \delta \gamma \sin 2\varphi}{\delta m_{21}^2} \left[ \frac{s_2}{s_1 c_1} \left( 1 + \frac{\delta m_{21}^2}{\delta m_{32}^2} \right) + \frac{c_2}{s_3} \frac{\delta m_{21}^2}{\delta m_{32}^2} \right], \quad (49)$$

in the limit  $\delta \rightarrow 0$ . Comparing this with the standard  $T$ -asymmetry,

$$\Delta P_T = \sin \delta \times \left\{ 16 s_1 c_1 s_2 c_2 s_3 c_3^2 \left[ \frac{1}{8E^3} \frac{\delta m_{12}^2 \delta m_{23}^2 \delta m_{31}^2}{\Delta_{12} \Delta_{23} \Delta_{31}} \right] \times \sin \frac{\Delta_{12} L}{2} \sin \frac{\Delta_{23} L}{2} \sin \frac{\Delta_{31} L}{2} \right\}, \quad (50)$$

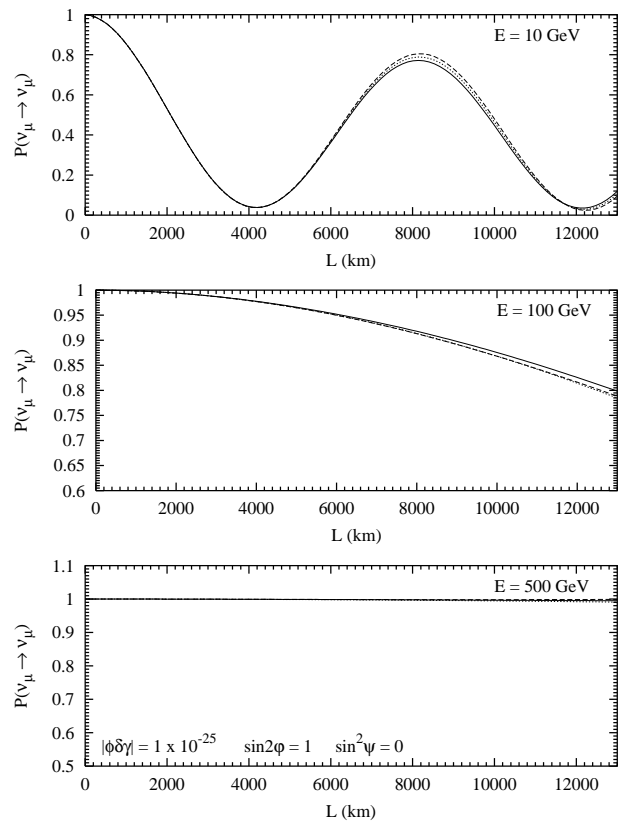


FIG. 9:  $\nu_\mu$  survival probability at various energies and  $|\phi|\delta\gamma = 1 \times 10^{-25}$ . Solid (dashed) lines are for maximal  $\nu_e \leftrightarrow \nu_\tau$  VEP mixing with a positive (negative)  $|\phi|\delta\gamma$ . Dotted lines are for the standard, no VEP case.

we see that the relative phase  $\beta$  can mimic the role of the standard phase  $\delta$ .

Assuming  $\delta = 0$ , Fig. 8 shows the  $T$ -trajectories for this case at  $E = 13$  GeV and  $|\phi|\delta\gamma = 1 \times 10^{-25}$ , with  $\beta$  as the phase variable. Because of the factor  $Q$ , the shape of these  $T$ -trajectories can be quite different from the standard  $T$ -trajectories (as functions of  $\delta$ ), which are displayed also in the same figure.

### VI. COMPATIBILITY WITH THE SUPER-KAMIOKANDE ATMOSPHERIC NEUTRINO DATA

Since the sensitivity of an experiment to VEP-LIV increases with  $L \cdot E$ , it is instructive to reexamine our case in the light of the Super-Kamiokande atmospheric neutrino data, whose parent neutrino distribution spans some four decades in neutrino energy,  $E \sim 0.1 \rightarrow 10^3$  GeV. We do not have the technology to perform a full-fledged three-flavour fit to the data to ensure that the VEP parameters considered in this work are not in conflict with experimental data. However, the same purpose may be more than amply achieved by requiring the new  $\nu_\mu$  survival probabilities not to deviate too much from that given by

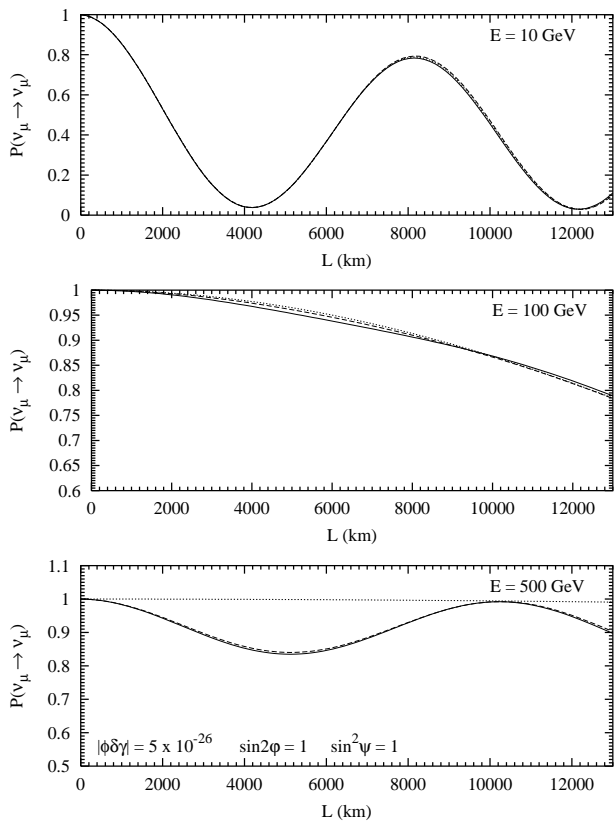


FIG. 10: Same as Fig. 9, but for  $|\phi\delta\gamma| = 5 \times 10^{-26}$  and maximal  $\nu_e \leftrightarrow \nu_\mu$  VEP mixing.

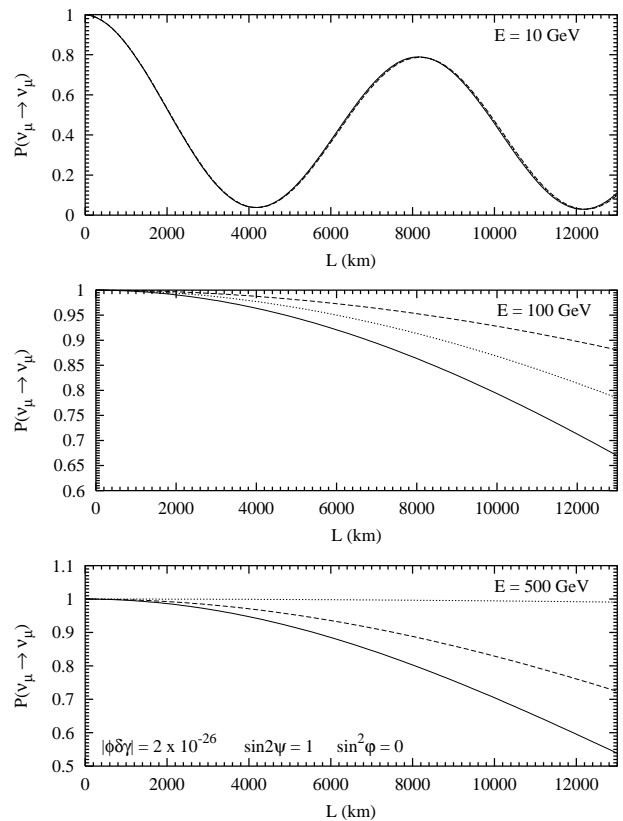


FIG. 11: Same as Fig. 9, but for  $|\phi\delta\gamma| = 2 \times 10^{-26}$  and maximal  $\nu_\mu \leftrightarrow \nu_\tau$  VEP mixing. According to Ref. [12], the solid and dashed curves are allowed by the Super-Kamiokande atmospheric neutrino data.

the best fit parameters.

Figures 9 and 10 show the  $\nu_\mu$  survival probability at several energies, with maximal VEP mixing in the  $(\nu_e, \nu_\tau)$  and  $(\nu_e, \nu_\mu)$  sectors respectively. In the case of  $\nu_e \leftrightarrow \nu_\tau$  VEP mixing, there is virtually no deviation from the standard  $\nu_\mu$  survival probability at  $E = 10, 100,$  and  $500$  GeV for  $|\phi\delta\gamma| = 1 \times 10^{-25}$ . The case of  $\nu_e \leftrightarrow \nu_\mu$  VEP mixing seems somewhat more restricted. At  $E = 500$  GeV and  $|\phi\delta\gamma| = 5 \times 10^{-26}$ , the departure from the standard probability can be as large as  $\sim 15\%$ . However, bearing in mind that the neutrino source peaks at  $\sim 100$  GeV, this divergence at 500 GeV is most likely still acceptable. The case of VEP mixing in the  $(\nu_\mu, \nu_\tau)$  sector was considered in Ref. [12] in a two-flavour analysis. For the purpose of comparison, we plot in Fig. 11 the  $\nu_\mu$  survival probability for a  $|\phi\delta\gamma|$  just above the upper limit of  $10^{-26}$  from the said analysis. Clearly, the curves in Figs. 9 and 10 are no worse than these “acceptable” ones. Thus we can be quite confident that the VEP parameters considered in this work have not already been ruled out by Super-Kamiokande. A proper analysis is required to settle this issue.

## VII. CONCLUSION

We have considered in this work the prospects for extending the limits on equivalence principle and Lorentz invariance violations (VEP and LIV) in future neutrino factory experiments. We have examined three neutrino flavour oscillations, treating VEP-LIV as a sub-leading mechanism to the standard mass-mixing mechanism, under the simplifying assumption that the neutrino-gravity couplings of two of the three neutrino gravitational eigenstates are nearly the same. The presence of nondegenerate neutrino-gravity couplings introduces additional mixing and phases which can lead to  $CP$ - and  $T$ -violation even if the phase  $\delta$  in the MNS mixing matrix vanishes.  $T$ -violation measurements have the potential to yield the most stringent bounds on VEP-LIV. Our case study shows that, with suitable neutrino path lengths of several thousand kilometres, the limits on VEP-LIV for the  $(\nu_e, \nu_\mu)$  and  $(\nu_e, \nu_\tau)$  sectors can be lowered to  $|\phi\delta\gamma| \lesssim 10^{-26}$ , which matches the limit for the  $(\nu_\mu, \nu_\tau)$  sector imposed by the Super-Kamiokande atmospheric neutrino data. At present, we see little prospect for extending this limit much beyond the  $10^{-26}$  level.

### Acknowledgments

This work was supported in part by the U. S. Department of Energy under grant DE-FG02-84ER40163.

C.N.L. would like to thank S. M. Barr, I. Dorsner, and A. Halprin for useful discussions.

- 
- [1] M. Gasperini, Phys. Rev. D **38**, 2635 (1988); **39**, 3606 (1989).
  - [2] A. Halprin and C. N. Leung, Phys. Rev. Lett. **67**, 1833 (1991); J. Pantaleone, A. Halprin, and C. N. Leung, Phys. Rev. D **47**, R4199 (1993).
  - [3] S. Coleman and S. L. Glashow, Phys. Lett. B **405**, 249 (1997); Phys. Rev. D **59**, 116008 (1999).
  - [4] S. L. Glashow, A. Halprin, P. I. Krastev, C. N. Leung, and J. Pantaleone, Phys. Rev. D **56**, 2433 (1997).
  - [5] CCFR Collaboration, A. Romosan *et al.*, Phys. Rev. Lett. **78**, 2912 (1997).
  - [6] J. Pantaleone, T. K. Kuo, and S. W. Mansour, Phys. Rev. D **61**, 033011 (2000).
  - [7] C. Athanassopoulos *et al.*, Phys. Rev. Lett. **75**, 2650 (1995).
  - [8] A. Halprin, C. N. Leung, and J. Pantaleone, Phys. Rev. D **53**, 5365 (1996).
  - [9] J. N. Bahcall, P. I. Krastev, and C. N. Leung, Phys. Rev. D **52**, 1770 (1995).
  - [10] S. W. Mansour and T. K. Kuo, Phys. Rev. D **60**, 097301 (1999).
  - [11] Super-Kamiokande Collaboration, Y. Fukuda *et al.*, Phys. Rev. Lett. **81**, 1562 (1998); Phys. Lett. B **433**, 9 (1998); Phys. Lett. B **436**, 33 (1998); Phys. Rev. Lett. **82**, 2644 (1999).
  - [12] G. L. Fogli, E. Lisi, A. Marrone, and G. Scioscia, Phys. Rev. D **60**, 053006 (1999).
  - [13] P. Lipari and M. Lusignoli, Phys. Rev. D **60**, 013003 (1999).
  - [14] A. M. Gago, H. Nunokawa, and R. Zukanovich Funchal, Phys. Rev. Lett. **84**, 4035 (2000).
  - [15] A. M. Gago, M. M. Guzzo, P. C. de Holanda, H. Nunokawa, O. L. G. Peres, V. Pleitez, and R. Zukanovich Funchal, Phys. Rev. D **65**, 073012 (2002).
  - [16] A. Raychaudhuri and A. Sil, Phys. Rev. D **65**, 073035 (2002).
  - [17] B. T. Cleveland *et al.*, Astrophys. J. **496**, 505 (1998).
  - [18] SAGE Collaboration, V. N. Gavrin, Nucl. Phys. B (Proc. Suppl.) **91**, 36 (2001).
  - [19] GALLEX Collaboration, W. Hampel *et al.*, Phys. Lett. B **447**, 127 (1999).
  - [20] GNO Collaboration, M. Altmann *et al.*, Phys. Lett. B **490**, 16 (2000).
  - [21] Kamiokande Collaboration, Y. Fukuda *et al.*, Phys. Rev. Lett. **77**, 1683 (1996).
  - [22] Super-Kamiokande Collaboration, S. Fukuda *et al.*, Phys. Rev. Lett. **86**, 5651 (2001).
  - [23] SNO Collaboration, Q. R. Ahmad *et al.*, Phys. Rev. Lett. **87**, 071301 (2001).
  - [24] KamLAND Collaboration, K. Eguchi *et al.*, hep-ex/0212021.
  - [25] C. Albright *et al.*, hep-ex/0008064.
  - [26] A. Bueno, M. Campanelli, S. Navas-Concha, and A. Rubbia, Nucl. Phys. **B631** 239 (2002).
  - [27] T. K. Kuo and J. Pantaleone, Phys. Lett. B **198**, 406 (1987); P. I. Krastev and S. T. Petcov, *ibid.* **205**, 84 (1988).
  - [28] E. K. Akhmedov, P. Huber, M. Lindner, and T. Ohlsson, Nucl. Phys. **B608**, 394 (2001).
  - [29] See, for example, A. Datta, Phys. Lett. B **504**, 247 (2001).
  - [30] Z. Maki, M. Nakagawa, and S. Sakata, Prog. Theor. Phys. **28**, 870 (1962).
  - [31] See, for example, M. C. González-García, M. Maltoni, C. Peña-Garay, and J. W. F. Valle, Phys. Rev. D **63**, 033005 (2001).
  - [32] C. Jarlskog, Z. Phys. C **29**, 491 (1985); Phys. Rev. Lett. **55**, 1039 (1985).
  - [33] V. A. Naumov, Int. J. Mod. Phys. **D1**, 379 (1992); P. F. Harrison and W. G. Scott, Phys. Lett. B **476**, 349 (2000).
  - [34] H. Minakata and H. Nunokawa, JHEP **0110**, 001 (2001).
  - [35] H. Minakata, H. Nunokawa, and S. Parke, Phys. Lett. B **537**, 249 (2002).